Understanding Zinc(II) Chelation with Quercetin and Luteolin: A Combined NMR and Theoretical Study

ARTICLE *in* THE JOURNAL OF PHYSICAL CHEMISTRY B · DECEMBER 2014

Impact Factor: 3.3 · DOI: 10.1021/jp509752s · Source: PubMed

6 AUTHORS, INCLUDING:

Christina Lekka
University of Ioannina
9 PUBLICATIONS **88** CITATIONS
SEE PROFILE

Nino Russo
Università della Calabria
511 PUBLICATIONS **7,941** CITATIONS
SEE PROFILE

Ioannis P Gerothanassis
University of Ioannina
146 PUBLICATIONS **2,682** CITATIONS
SEE PROFILE

THE JOURNAL OF PHYSICAL CHEMISTRY B

Article

pubs.acs.org/JPCB

Understanding Zinc(II) Chelation with Quercetin and Luteolin: A Combined NMR and Theoretical Study

Alexandra Primikyri,[†] Gloria Mazzone,*[,‡] Christina Lekka,[§] Andreas G. Tzakos,[†] Nino Russo,[‡,⊥] and Ioannis P. Gerothanassis*[,†]

[†]Department of Chemistry, University of Ioannina, Ioannina, GR-45 110, Greece

[‡]Dipartimento di Chimica e Tecnologie Chimiche, Università della Calabria, I-87036 Arcavacato di Rende, Italy

[§]Department of Material Science Engineering, University of Ioannina, Ioannina, GR-45 110, Greece

[⊥]Departamento de Quimica, Division de Ciencias Basicas e Ingenieria, Universidad Autonoma Metropolitana-Iztapalapa, Avenue San Rafael Atlixco No. 186, Col. Vicentina, CP 09340, Mexico, D.F. Mexico

Supporting Information

ABSTRACT: The Zn(II) chelation with natural flavonoids, quercetin and luteolin, was investigated by the use of NMR spectroscopy and various levels of ab initio calculations. Very sharp phenolic OH ^{1}H resonances in DMSO-d_6 were observed for both free and complexed quercetin which allowed (i) the unequivocal assignment with the combined use of $^{1}H-^{13}C$ HSQC and HMBC experiments and (ii) the determination of complexation sites which were found to be the CO-4 carbonyl oxygen and the deprotonated C-5 OH group of quercetin and CO-4 carbonyl oxygen and the deprotonated C-5 OH group of luteolin. DOSY experiments allowed the determination of the effective molecular weight of the Zn−quercetin complex which was shown to be mainly 1:1. DFT calculations of the 1:1 complex in the gas phase demonstrated that the C-3 O^- and CO-4 sites are favored for quercetin at both GGA and LDA approximations and the C-5 O^- and CO-4 groups of luteolin at the LDA approximation. Quantum chemical calculations were also performed by means of the conductor polarizable model in DMSO by employing various functionals. The energetically favored Zn chelation sites of the 1:1 complex were found to be either the C-3 O^- and CO-4 or C-5 O^- and CO-4 sites, depending on the functional used, for quercetin and the C-5 O^- and CO-4 sites for luteolin.

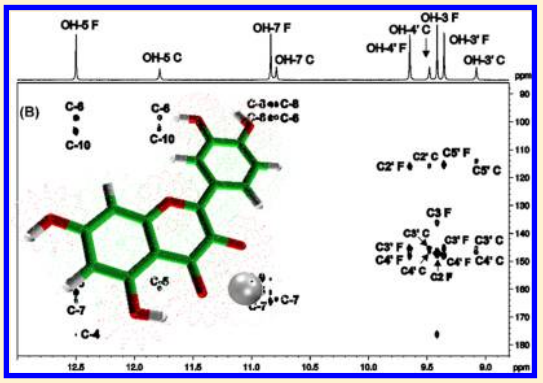

1. INTRODUCTION

Numerous experimental and clinical investigations suggested that flavonoids, as natural dietary phytochemicals, are potential cardioprotective, neuroprotective and chemopreventive agents.[1] There have been more than 8000 flavonoids characterized, and this number is constantly growing due to their great structural diversity. They are subdivided into several families, e.g. flavones, flavonols, flavanones, isoflavones, flavan 3-ols, flavanonols and anthocyanins. The differences in the number and the distribution of the hydroxyl groups across the three rings (Scheme 1) as well as their substitutions are responsible for their wide range of biological effects as well as for their antioxidant activities.[2]

It is commonly accepted that the most essential structural characteristics which provide effective antioxidant activity are the presence of (i) phenolic OH groups in ortho-position, (ii) a double bond between C-2 and C-3 and (iii) additional functional groups like the C═O carbonyl group. Also the presence of a 3-hydroxyl group in the heterocyclic ring C increases the radical-scavenging activity of flavonols, while an additional hydroxyl group on the B ring was reported to increase the antioxidant activity.[3]

Currently there is a no available unified mode of action of antioxidant activity of flavonoids. On the contrary different groups have published contradicted biological results and hypothesis on the same molecules. The three main molecular mechanisms which are suggested are the H donation, the single electron transfer and the metal chelation. In particular the first two proposed mechanisms are referred to free radical scavenging activity, for example, by limiting the production of reactive oxygen species (ROS) and/or scavenging them, inhibiting lipid peroxidation and low density lipoprotein (LDL) oxidation.[4] The presence of −OH groups is also potentially important to "chelate" the free labile iron that is present in the cellular matrix and induce oxidative damage. Several studies support the hypothesis that flavonoids bind iron and, thus, inhibit the catalysis of Fenton reaction which produces hydroxyl radicals which are extremely damaging to cells.[5]

Received: September 26, 2014
Revised: December 5, 2014
Published: December 8, 2014

   dx.doi.org/10.1021/jp509752s | J. Phys. Chem. B 2015, 119, 83−95

Scheme 1. Potential Chelation Sites of Metals with Site 1 Demonstrating Higher Affinity Followed by Sites 2 and 3

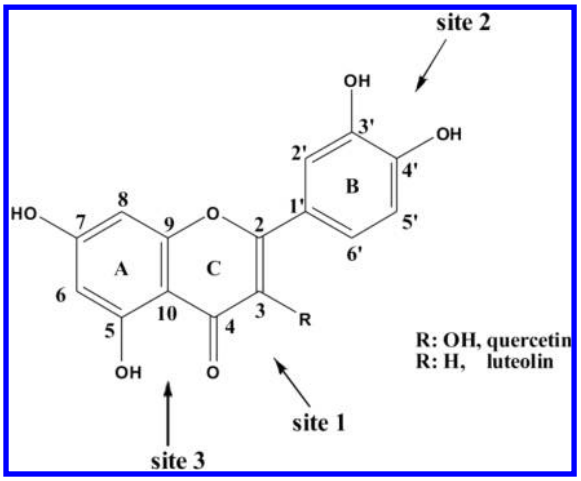

Several theoretical and experimental studies have been performed in order to study the metal complexation mechanism of various flavonoids. For example, DFT studies demonstrated that the 3-hydroxyl-4-carbonyl group is the optimal chelation site for Fe, while the 4−5 and 3′−4′ groups are less favorable complexation sites.[6] DF-B3LYP studies on the chelation of Fe(II) by quercetin indicated that both neutral and deprotonated forms of quercetin can give stable complexes with bare and hydrated Fe(II) with the 1:2 stoichiometry providing the most stable one. Positions 3−4 and 4−5 were determined as the most favored coordination sites for Fe(II) complexation.[7] Other DFT and molecular dynamics calculations for Fe^{+} and Cu^{+} indicated their preference for chelating ring C and in particular the 4-carbonyl oxygen when there is no substituent in position 3.[8]

The iron-binding properties of several flavonoids were investigated in aqueous media by various spectroscopic techniques. Quercetin was found to bind Fe^{2+} with the 3-hydroxyl-4-carbonyl site providing the most preferable chelating position.[9] Several metal complexes of quercetin were characterized by Zhou et al.[10] by the use of various experimental techniques and indicated that the C-3 OH group is deprotonated with the complexation site located at the C-3 O^{-} group and the CO-4 carbonyl.

Zinc is an essential element and plays a pivotal role in various metabolic and signaling pathways, cell proliferation and apoptosis, defense against free radicals and oxidative stress and DNA damage repair. Zn(II), which is not an oxidizing agent for phenolic groups and instead acts as a Lewis acid, has antagonistic role in redox active bivalent transition metals including iron and copper and prevents the deleterious free-radical reactions (e.g., Fenton reaction) stimulated by iron and copper.[11] Nevertheless, there is a limited number of studies in the literature. Lapouge et al. explored the complexation of Zn(II) by 3-hydroxyflavone, 5-hydroxyflavone and 3′,4′-dihydroxyflavone which result in the formation of complexes of 1:1 stoichiometry.[12] Spectroscopic studies deduced that two Zn ions chelate quercetin; the C-3 OH and CO-4 coordinating sites were found to be of high activity whereas OH-3′ on ring B of lower affinity.[13] Other experimental studies about Al(III) and Zn(II) complexes with flavonoids also confirmed that the chelation sites for quercetin are C-3 OH and 4-oxo groups, whereas C-3′, C-4′ OH groups bound a second metal ion.[14]

The aim of the present work was to investigate the complexation of Zn(II) ions with two representative flavonoids, quercetin and luteolin, with the combined use of NMR and first-principle calculations.

2. METHODS

2.1. NMR. NMR experiments were performed using a Brüker AV-500 spectrometer equipped with a TXI cryoprobe (Brüker BioSpin, Rheinstetten, Germany) and using a Brüker AV-400 spectrometer. Samples were dissolved in 0.6 mL of deuterated solvent and transferred to 5 mm NMR tubes. Chemical shifts were measured with the reference to the internal standard $Me_3SiCD_2CD_2COONa$, TSP-d_4 (δ_H = 0.00 ppm). The 2D $^{1}H-^{13}C$ HSQC and HMBC experiments were carried out using standard software and parameters were optimized for coupling constants of 145.0 and 8.0 and 2.5 Hz, respectively. To ensure adequate relaxation of the OH protons used for the integration of the free and bound state of quercetin, their T_1s were measured using the inversion recovery pulse sequence. T_1s were found to be 2.5−3.0 s, thus, the pulse repetition time was set at ∼4 T_1s of the longest T_1 value. DOSY experiments were performed with the bipolar pulse longitudinal eddy current delay (BPPLED) pulse sequence.[15] 16 BPPLED spectra with 16K data points were collected and the eddy current delay was set to 5 ms. The complex of quercetin with Zn(II) was prepared with titration of $ZnCl_2$ (200 mM) in a solution of Quercetin anhydrous (7 mM) in DMSO-d_6. Respectively, $ZnCl_2$ (108 mM) was titrated into a 1 mM solution of luteolin (1 mM) in DMSO-d_6.

2.2. DFT Calculations. Calculations were performed in the framework of density functional theory employing different exchange-correlation functionals. The Ceperley−Alder form (as parametrized by Perdew and Zunger) of the local density approximation (LDA)[16] and the Perdew−Burke−Ernzerhorf of the generalized gradient−corrected approximation (GGA)[17] were used in conjugation with norm-conserving Troullier−Martins type pseudopotentials[18−20] to model the atomic cores and a basis of double-ζ polarized orbitals (13 atomic orbitals for C, N, and O, 5 orbitals for H and 25 orbitals for Zn) by means of the SIESTA code.[21−23] In the optimization calculations, an auxiliary real space grid equivalent to a plane-wave cutoff of 100 Ry was used and the structure was considered fully relaxed when the magnitude of forces on the atoms was found smaller than 0.04 eV/Å.

Starting structures of the complexes were constructed chelating the Zn atom close to the 3−4, 4−5, and 3′−4′ sites of quercetin or near the 4−5 and 3′−4′ sites of luteolin, abstracting selectively H atoms from the corresponding OH groups. Furthermore, since $ZnCl_2$ was used in the NMR experiments, selected complexes solvated by chlorine were also considered in the absence or presence of a H_2O molecule and the corresponding E_b and $E_{b'}$ were calculated adding the appropriate species in eqs 1 and 2.

For the complex binding energy calculation, it was necessary to account for the changes in the flavonoid structure due to the removal of H atoms from OH groups where the Zn atom was bound.[6,24] Therefore, two choices for the relevant chemical potentials for the abstracted H atoms were considered: the first H reservoir corresponds to H_2 molecules and the second to H_2O molecules. These two choices, although they may appear as oversimplifications, correspond approximately to the limited cases of acidic and basic solutions.[6,24] The corresponding complex binding energies (E_b and $E_{b'}$) are defined as

dx.doi.org/10.1021/jp509752s | J. Phys. Chem. B 2015, 119, 83−95

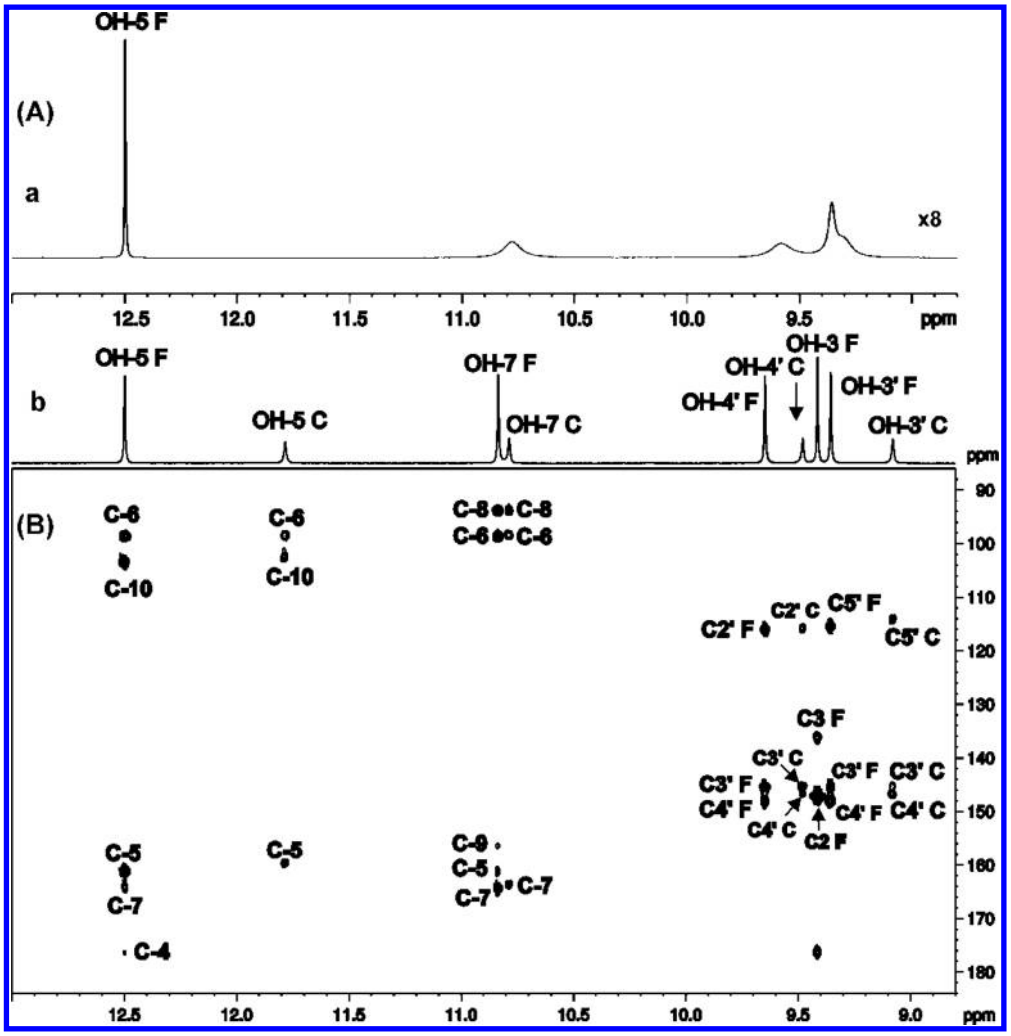

Figure 1. Selected regions of the 500 MHz (A) 1H NMR spectra of quercetin, 7 mM in DMSO-d_6 (a); (b) as in part a in the presence of 200 mM of Zn(II) (T = 298 K, number of scans =8, experimental time =1 min). (B) 2D $^{1}H-^{13}C$ HMBC NMR spectrum of the solution of part A(b) (T = 298 K, number of scans =88, total experimental time =11 h 30 min). F and C denote free and complexed quercetin, respectively.

$$E_b = E_{total} - n_{Zn}E_{Zn} - n_{Que}E_{Que} + n_H E_H + n_H \frac{1}{2} E_{H_2} \quad (1)$$

$$E_b' = E_{total} - n_{Zn}E_{Zn} - n_{Que}E_{Que} + n_H E_H + n_H \frac{1}{2}(E_{H_2O} - E_H - E_{OH}) \quad (2)$$

where E_{total} is the total energy of the complex and E_X, n_X, are the energy and number of species X involved in the complexation reaction (X = Zn, Que (or Lut), H); in particular, n_H is the number of H atoms missing from the neutral quercetin (or luteolin) molecules after complexation, and E_{H_2} is the binding energy per H_2 molecule, while for the second reservoir, the abstracted H atoms become part of a H_2O molecule.[6,24]

In addition to such calculations, Gaussian 09 computational package[25] was used to explore all the possible Zn(II)-flavonoid complexes, by employing two hybrid exchange and correlation functionals, B3LYP[26,27] and M05-2X,[28] and one range-separated hybrid functional wB97XD,[29] which includes empirical dispersion. The 6-31+G* basis set of Pople has been used for all the atoms, except for the Zn atom, for which the relativistic compact Stuttgart/Dresden effective core potential[30] was used in conjunction with its split valence basis set. Harmonic vibrational frequencies have been performed to characterize all the investigated compounds as minima. The structures have been fully optimized at each level of theory, while final energies have been calculated by performing single-point calculations on the optimized geometries at the same level of theory and employing the larger 6-311++G** standard basis set for all the atoms and the SDD pseudopotential for the Zn atom, taking into account also the impact of the solvent used in the experiments, DMSO (ε = 46.826), by means of the conductor polarizable continuum model (CPCM)[31] as implemented in Gaussian 09. The UAHF set of radii has been used to build-up the cavity. In the case of M05-2X the SMD continuum model[32] has been used to mimic the solvent environment.

In addition, single point energies on the optimized geometries with the M05-2X functional have been computed at the MP2 level through the RI-MP2[33] approach as implemented in the TURBOMOLE program package[34] (version 6.3) in conjunction with the same relativistic Stuttgart/Dresden pseudopotential for zinc and the standard internally stored TZVP basis set[35,36] for the rest of the atoms.

A further optimization has been carried out at the B3LYP/6-311++G** level. Such geometries and those obtained by the optimization at B3LYP/6-31+G* level of theory have been

dx.doi.org/10.1021/jp509752s | J. Phys. Chem. B 2015, 119, 83−95

used to estimate the absolute chemical shielding of the most stable complexes of Zn(II) with both quercetin and luteolin in implicit DMSO, by using the gauge-independent atomic orbital (GIAO) method,[37,38] as implemented in the Gaussian 09 package. Chemical shifts have been then obtained from absolute shieldings by subtraction of a calculated reference. The absolute chemical shielding of TMS, computed at each level of theory, have been used for this purpose.

3. RESULTS AND DISCUSSION

3.1. NMR Studies. *3.1.1. Resonance Assignment: ^{1}H, ^{1}H−^{13}C HSQC, and HMBC Experiments.* The 1D ^{1}H NMR spectrum of quercetin (7 mM) in DMSO-d_6 exhibits a sharp and extremely deshielded resonance at 12.51 ppm (Figure 1A) which can be attributed to the C-5 OH proton that participates in a strong intramolecular hydrogen bond with the CO-4 carbonyl oxygen atom.[39] In contrast the C-3, C-3′, and C-4′ OH resonances appear as extremely broad resonances in the region of 9.2−9.7 ppm while the C-7 OH group cannot be distinguished from the baseline due to intermolecular proton exchange with traces of H_2O in the organic solvent. This exchange rate depends on the concentration of the solute molecule and of the residual H_2O and it is acid- or base-catalyzed.[40] Recently, it has been demonstrated that a significant line width reduction was observed in phenolic hydrogen group with the addition of various acids such as HCl,[41] CCl_3COOH, CF_3COOH, and picric acid.[42] The optimum line width reduction by a factor of over 100 was observed with the addition of picric acid which resulted in line widths ≤2 Hz.

The ^{1}H NMR spectrum of quercetin in the presence of Zn(II) (200 mM) in DMSO-d_6 demonstrates very sharp and distinct resonances for both free and Zn(II) bound quercetin. The significant reduction in the phenol OH line widths could probably be attributed to the release of HCl upon the addition of $ZnCl_2$ and, thus, change the pH resulting in the reduction of proton exchange rate. Application of the 2D ^{1}H−^{13}C HMBC method (Figure 1B) demonstrated a significant number of $^nJ(^1H,^{13}C)$ cross-peaks of the hydroxyl groups which, in combination with the 2D ^{1}H−^{13}C HSQC spectrum, allowed the assignment of both the free and Zn-complexed quercetin (Table 1).

Table 1. ^{1}H and ^{13}C Chemical Shifts for the Free and Complexed Form of Quercetin with Zn(II)

proton	free	complex	carbon	free	complex
OH5	12.51	11.80	C2	147.2	
OH7	10.85	10.78	C3	136.0	145.1
OH4′	9.65	9.49	C4	176.5	178.0
OH3	9.42	–	C5	161.4	160.1
OH3′	9.36	9.08	C6	98.8	98.6
H2′	7.68	7.93	C7	164.2	163.7
H6′	7.55	7.97	C8	93.9	93.7
H5′	6.88	6.84	C9	156.4	159.8
H8	6.41	6.43	C10	103.7	102.9
H6	6.19	6.19	C1′	122.3	125.07
			C2′	115.3	114.2
			C3′	145.5	145.7
			C4′	148.0	146.8
			C5′	115.4	114.2
			C6′	120.2	119.5

The deprotonation of the C-3 OH group and the significant deshielding upon complexation of the C-3 carbon (∼9 ppm) and C-4 carbon (∼2 ppm) clearly demonstrate that C-3 OH and CO-4 functional groups are the coordination sites (Table 1). It should be emphasized that although a substantial number of publications have been concerned with complexation of diamagnetic and paramagnetic metal ions with ligands particularly with the use of heteronuclear NMR,[43,44] this is the first demonstration of a slow exchange on the NMR time scale of free and bound ligands with the use of the OH ^{1}H NMR spectral region.

Similar experiments performed for luteolin (Figure 2), demonstrated the deprotonation of the C5 OH group. 2D ^{1}H−^{13}C HMBC (Figure 2B) 2D ^{1}H−^{13}C HSQC spectra allowed the assignment of both the free and Zn-complexed luteolin (Table 2). Interestingly, the deprotonation sites for quercetin (C3 OH) and luteolin (C-5 OH) upon complexation with Zn(II) are the least acidic. Thus, for quercetin, pK_a for C3 OH was found between 11.26 to 11.56 and for C5 OH at ∼13.06. These values should be compared with pK_a in the range of 8.62 to 9.44 for C7 OH, C3′ OH, C4′ OH groups.[45]

3.1.2. Variable Temperature NMR Experiments. It has been demonstrated that the temperature dependence of ^{1}H NMR chemical shifts of phenol OH groups is linear and the derived $\Delta\delta/\Delta T$ coefficients span a range of −0.5 to −12.3 ppb K^{-1} in DMSO-d_6, acetone-d_6, and CD_3CN solution.[46−48] $\Delta\delta/\Delta T$ values in DMSO-d_6, with the exception of C-5 OH of flavonoids, are in the range of −5.4 to −8.0 ppb K^{-1} when reference is made to the solvent peak (−5.8 to −8.4 ppb K^{-1} when reference is made to the internal standard TMSP-d_4). This range of $\Delta\delta/\Delta T$ values implies that all the phenol −OH groups are exposed to the solvent and the OH groups in the ortho position, such as the C-3′ and C-4′ OH groups of quercetin, are not involved in intramolecular flip-flop hydrogen bond interactions.[49] $\Delta\delta/\Delta T$ values of C-5 OH were found to be significantly smaller in absolute terms (more positive than −2.5 ppb K^{-1}) than those of other hydroxyl protons which are exposed to the solvent, irrespective of the solvent used. This indicates that the C-5 OH is involved in a strong intramolecular hydrogen bond with the CO-4 oxygen atom. Because of strong intramolecular C-5 OH−OC4 hydrogen bond the surrounding solvent molecules around the C-5 hydroxyl proton are excluded leading to a significantly reduced solvation and a consequent small solvent and temperature dependence relative to the OH protons which are exposed to the solvent.[46−48]

Figure 3 illustrates that the temperature coefficient of the C-5 OH of the Zn-complex ($\Delta\delta/\Delta T$ =-2.9 ppb K^{-1}) is very similar to that of the free quercetin ($\Delta\delta/\Delta T$ = −2.2 ppb K^{-1}). This demonstrates that the strong C-5 OH−OC-4 intramolecular hydrogen bond persists also in the Zn(II) complex.

The equilibrium for the formation of the complex can be described by the equilibrium constant K_{eq}

$$K_{eq} = [Zn^{2+}]/[\text{quercitin}] \quad (3)$$

which is related to the free energy ΔG°

$$\Delta G^\circ = -RT \ln K_{eq} \quad (4)$$

Once the equilibrium constant has been determined at several temperatures, then, according to the Van't Hoff equation

$$\ln K_{eq} = -\Delta H^\circ/RT + \Delta S^\circ/R \quad (5)$$

dx.doi.org/10.1021/jp509752s | J. Phys. Chem. B 2015, 119, 83−95

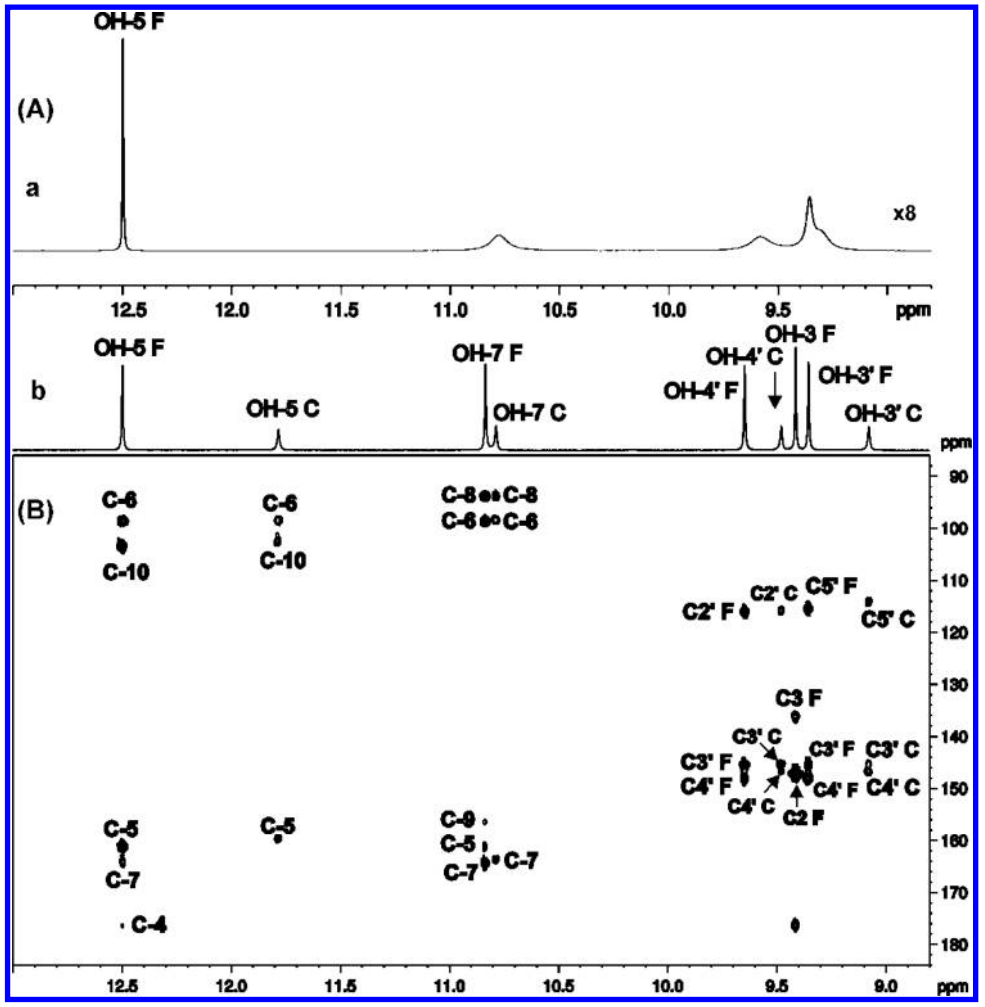

Figure 2. Selected regions of the 500 MHz (A) ^{1}H NMR spectra of luteolin, 1 mM in DMSO-d_6 (a); (b) as in part a in the presence of 108 mM of Zn(II) (T = 298 K, number of scans =8, experimental time =1 min). (B) 2D ^{1}H–^{13}C HMBC NMR spectrum of the solution of part A(b) (T = 298 K, number of scans =272, total experimental time = 11 h 33 min). F and C denote free and complexed quercetin, respectively.

Table 2. ^{1}H and ^{13}C Chemical Shifts for the Free and Complexed Form of Luteolin with Zn(II)

proton	free	complex	carbon	free	complex
OH5	13.03	–	C2	164.8	163.0
OH7	10.95	10.22	C3	104.5	107.3
OH3′	10.01	9. 95	C5	162.6	
OH4′	9.51	9.48	C6	99.8	
H2′	7.40	7.37	C7	164.9	164.6
H6′	7.43	7.37	C8	94.4	90.2
H5′	6.89	6.89	C9	158.2	160.2
H3	6.69	6.59	C10	104.1	103.6
H8	6.45	6.07	C1′	122.3	122.3
H6	6.21	5.87	C2′	116.9	116.9
			C3′	150.5	150.1
			C4′	146.6	146.7
			C5′	114.3	114.3
			C6′	119.9	119.4

the enthalpy of association (ΔH^{o}) and the corresponding entropy change (ΔS^{o}) can be determined. Two well resolved resonances of C5 OH_{free} and C5 OH_{bound}, were observed for a wide range of $[Zn^{2+}]/[quercetin]$ concentrations and over a sufficiently wide range of temperatures (288−338 K). This allowed the accurate determination of ln K_{eq} (Figure 4) and,

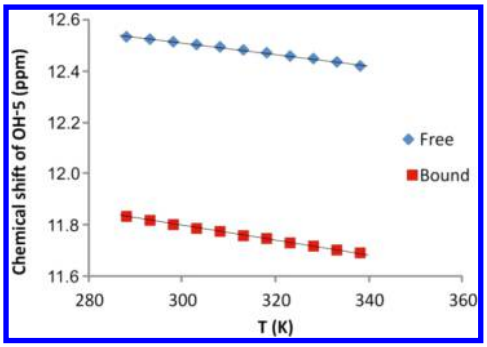

Figure 3. Temperature dependencies of the C-5 OH protons of free quercetin (blue ◆) and Zn(II)-complexed quercetin (red ■).

therefore, of ΔH^{o} and ΔS^{o}. For $[Zn^{2+}]/[quercetin]$ = 30, ΔH^{o} = 15.6 KJmol^{-1} and ΔS^{o} = 29.22 JK^{-1} mol^{-1}. At 298 K, $-T\Delta S^{o}$ = −8.92 kJ mol^{-1}. This demonstrates that the formation of Zn(II)-quercetin complex is enthalpically unfavorable presumably due to weak complexation, and is favored entropically due to release of HCl. Nevertheless, the variations of ΔH^{o} and ΔS^{o} for various ratios of $[Zn^{2+}]/[quercetin]$ and H_2O concentrations were found to be significant.

3.1.3. DOSY Experiments—Determination of the Effective MW. Over the past decade, pulsed field-gradient (PFG) NMR

dx.doi.org/10.1021/jp509752s | J. Phys. Chem. B 2015, 119, 83−95

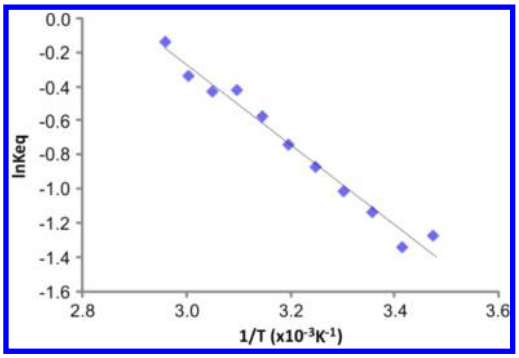

Figure 4. Representative Van't Hoff plot based on the equilibrium NMR integration data of the C-5 OH protons of quercetin for the formation of the Zn(II)−quercetin complex of the solution of Figure 1A(b). The solid line represents the best fit to eq 5

and diffusion ordered spectroscopy (DOSY) have been widely implemented in the study of molecular and the translational motion of both chemical and biological systems.[50] The self-diffusion coefficient D of a spherical molecule is described by the Stokes−Einstein equation

$$D = K_b T / 6\pi\eta r_s \quad (6)$$

where K_b is the Boltzmann constant, T is the absolute temperature, η is the viscosity of the medium, and r_s is the hydrodynamic radius. Thus, it provides information about the physicochemical properties of a given molecular species like size, shape and weight and furthermore allows detection of molecular interactions, including intermolecular interactions, aggregation and conformational changes.

The DOSY spectrum of free quercetin and Zn(II)−quercetin complex is illustrated in Figure 5. The diffusion coefficient of 2′

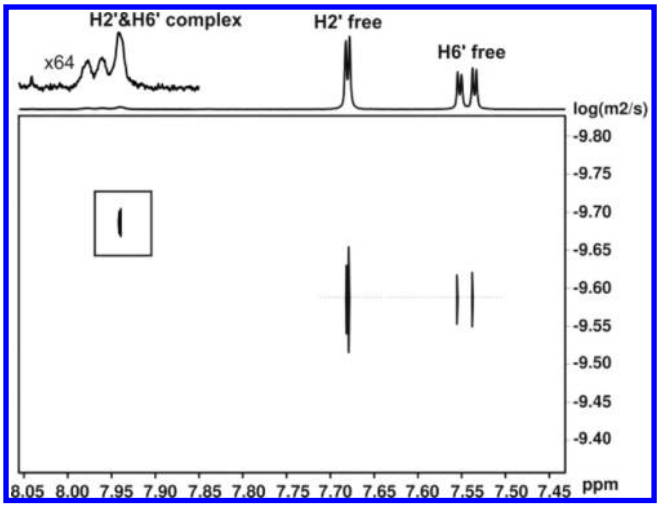

Figure 5. DOSY NMR spectrum of quercetin (3 mM) in the presence of 16 mM of Zn(II) in DMSO-d_6 (T = 298 K, number of scans = 8, total experimental time = 13 min).

and 6′ protons (D = 1.35 × 10^{-10} m^2 s^{-1}) of complex is decreased compared to the coefficient of the protons of free quercetin 2.15 × 10^{-10} m^2 s^{-1} for H2′ and 2.12 × 10^{-10} m^2 s^{-1} for H6′ protons, respectively. This is because of the increase in the molecular weight of the complex due to the metal chelation. Figure 6A illustrates a linear plot of the diffusion coefficients of TMS, DMSO-d_6, hexamethylocyclotrithyloxane (HMCT) and free quercetin with a correlation coefficient of 0.965. Inclusion

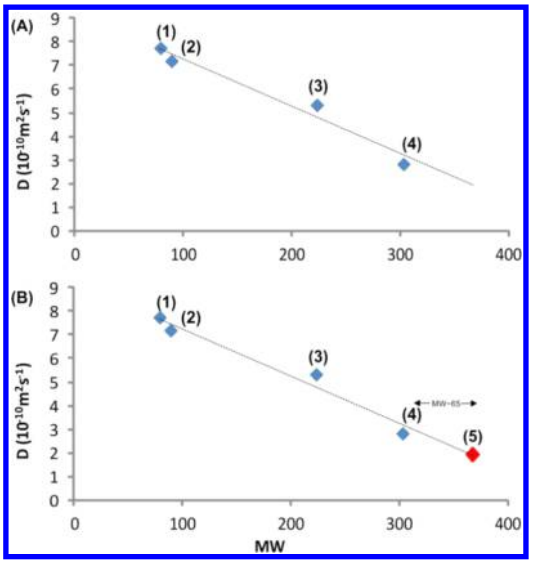

Figure 6. (A) Linear plot of the diffusion coefficients of DMSO (1), TMS (2), hexamethylocyclotrithyloxane (HMCT) (3), and quercetin free (4) of the solution of Figure 5 in which 3.4 mM of HMCT was added. (B) Diffusion coefficient of the Zn(II)−quercetin (5) complex included in the linear plot of part A.

of the diffusion coefficient of the Zn(II) complex in the linear plot of Figure 6A results in an effective molecular weight of the Zn^{2+} complex of ∼365 (Figure 6B) and, thus, the predominance of the 1:1 complex. To the best of our knowledge this is the first application of a DOSY experiment to investigate the effective molecular weight of a metal complex and, thus, may be of general utility in investigating metal−ligand complexation in solution.

3.2. DFT Calculations. DFT calculations were performed for the 1:1 Zn(II)-flavonoid complexes aiming in understanding the experimental results: (i) the preferred metal complexation site close to CO-4 carbonyl oxygen group, (ii) the deprotonation of the C-3 OH group of quercetin and the C-5 OH group of luteolin, and (iii) the experimentally observed C-5 OH−OC-5 intramolecular hydrogen bond as well as to reveal the Zn−quercetin bonding hybridizations.

In particular, both neutral and deprotonated complexes, see Scheme 1, were studied and the corresponding binding energies are presented in Table 3. For the Zn−quercetin complex, the 3−4 site deprotonated at the C-3 OH group is the favored one. This is in agreement with the NMR results and both Fe- and Cu−quercetin complexes.[6,24] The existence of H at the C-3 OH group results in a significant increase of the Zn−O bond distances, while the 3_H−4 binding energies for both reservoirs remain higher than the other complexes (Figure 7). The less favored complexation site is the 3′−4′ OH group in ring B. The chlorine reservoir increases the Zn coordination number and therefore the binding energy, while the presence of the H_2O ligand results in a more stable complex. For Zn−luteolin complexes, the 4−5 site was the favored one, Table 3, in agreement with the Fe− and Cu−luteolin complexes[24] while the 3_H′−4′ site is favored when GGA approximation is used. The presence of H at the C-5 hydroxyl group increases the binding energies and enlarges again the Zn−O distances. Upon chlorine addition, the binding energy of the complex increases significantly and the difference against the corresponding neutral case reaches 1 eV. The Zn−O distances are equivalent for all deprotonated complexes (Table 3) while the complexes

dx.doi.org/10.1021/jp509752s | J. Phys. Chem. B 2015, 119, 83−95

Table 3. Energies and Structural Parameters of Two Zn−Flavonoid Complexes[a]

		E_b (eV)		E_b' (eV)			
complex	site	GGA	LDA	GGA	LDA	N	d_{Zn-O} (Å)
Zn−Que	3−4	1.337	1.499	1.628	1.337	2	2.00
	3_H−4	0.587	1.420	0.877	1.258		2.92 (O_3), 2.69 (O_4)
	4−5	1.019	0.764	1.309	0.602	2	1.98
	4−5_H	0.587	0.866	1.083	0.704		2.82 (O_4), 2.65(O_5)
	3′−4′	0.007	0.219	0.588	0.057	2	1.93
	3_H′−4′	0.669	0.888	0.960	0.721	1	2.20(O_3′), 1.91(O_4′)
	3′−4_H′	1.124	1.014	1.414	0.852	1	1.91 (O_3′), 2.20 (O_4′)
	reservoir	Cl^-		Cl^-−H_2O			
	3−4	2.393	2.563	3.955	3.203	3, 4*	1.98
	3_H−4	1.203	1.174	2.786	1.877	3, 4*	2.08 (O_3), 1.90 (O_4)
Zn−Lut	4−5	0.102	0.726	0.393	0.564	2	1.92
	4−5_H	0.360	0.802	0.652	0.640		2.55 (O_4), 2.74 (O_5)
	3′−4′	−0.070	0.051	0.511	−0.110	2	1.93
	3_H′−4′	0.385	0.694	0.675	0.532	1	2.22 (O_3′), 1.90 (O_4′)
	3′−4_H′	0,284	0.642	0.574	0.480	1	1.90 (O_3′), 2.23 (O_4′)
	reservoir	Cl^-		Cl^-−H_2O			
	4−5	2169	1.606	3.731	2.281	3, 4*	1.92
	4−5_H	1113	0.543	2.614	1.164	3, 4*	1.83 (O_4), 2.11 (O_5)

[a]Zn binding energies (E_b and E_b', with respect to different reservoir choices for the abstracted H atoms, see text). H atoms are removed from the OH binding sites unless denoted with a subscript H. Average Zn−O distances; otherwise the corresponding O atom is given. N coordination number of Zn, where * stands for the H_2O case.

are almost planar with the dihedral angle intercepted by the C3, C2, C1′ and C6′ atoms to be between 0.5 and 1.6 deg.

Furthermore, the electronic wave functions for the Zn−quercetin complex of the energetically favored 3−4 site either solvated by chlorine or not were investigated aiming to understand (i) the electronic origin of the binding energy increase upon deprotonation or because of the chlorine-based reservoir and (ii) the experimentally observed C-5 OH−OC-4 intramolecular hydrogen bond. In Figure 7, selected wave functions (WF) are illustrated for the Zn−quercetin complexes. For the 3_H cases, the WF with similar charge distribution with the deprotonated ones are presented for comparison. Interestingly the deprotonated cases, around −5 eV, manifest a hybrid orbital that binds the C-5 OH group with the CO-4 one (named hereafter C-5 OH−OC-4) that is related to the strong C-5 OH−OC-4 intramolecular hydrogen bond that was observed experimentally. These states exhibit charge distribution in the neighborhood of both A and C rings, revealing mainly the σ-type bonding between Cp electrons, with the participation of the Znd electrons. Moreover, the chlorine reservoir introduces Zn d−Cl p electron hybridizations where the O_4 or the H_2O molecule may contribute (indicated by arrows), while energy states with charge located basically between the Zn−Cl atoms were also found. The Zn−quercetin bonding hybridizations are mainly found within the energy range of −3 and −4 eV. In Figure 7a, one lobe of the O_4 p orbital is hybridized with two lobes of the same sign Zn d orbital forming the enhanced red hybrid orbital (named O_4−Zn). In addition, at this WF C p−C p σ-like bonding was also found, while the chlorine reservoir reveals Zn d−Cl p hybridizations that are also depicted around −3.50 eV for the ZnCl−H_2O:quercetin case. The 3_H presence yields antibonding features between the O_4 and the Zn atoms for the Zn:quercetin-3_H case, while in the chlorine ligand cases both O_4 p−Zn d and Zn d−Cl p hybrid orbitals persist, although depleted. It is worth of note that O_4−Zn−Cl hybridizations were also found at lower energies enhancing therefore the O_4−Zn in the presence of Cl compared to the pure Zn−quercetin, in line with the increase of the corresponding binding energy (Table 3). For energies close to the Fermi level (0.0 eV), the WF are either distributed on quercetin manifesting the characteristic C p−C p and C p−O p π-like bond or they are located around the Zn atom revealing antibonding states between Zn and the closest O or Cl atoms; the presence of 3_H does not significantly alter these characteristics.

Summarizing: (i) the Zn chelation site in chlorine reservoir was found to be the CO-4 carbonyl oxygen and the deprotonated C-3 OH group for the quercetin complex (site 3−4, Table 3) or the deprotonated C-5 OH group (site 4−5, Table 3) for the luteolin complex compared to the neutral cases and the other reservoirs (using both LDA and GGA approximations) in line with the NMR experimental results; (ii) the enhanced binding energy of the chlorine's reservoir could be related to the Cl−Zn hybridizations that shift the energy states toward lower energies and (iii) the experimentally observed C-5 OH−OC-4 intramolecular hydrogen bond was found below −5.5 eV (far from E_F), the Zn−quercetin bonding states were found around −3.5 eV while antibonding states exist only close to the E_F.

The comparison of the obtained results (within the LDA approximation) on the Zn−flavonoids with the corresponding Fe or Cu complexes,[6,24] revealed that (a) all metals prefer the quercetin's chelation site 3−4, while the site 4−5 is favored in the case of luteolin's complexes, (b) all metals are more tightly bound with quercetin than to luteolin and (c) the binding energies of both Zn-flavonoid complexes are lower (at least by 0.5 eV) than the corresponding Fe and Cu ones'. This denotes that in the presence of Zn and Fe in the neighborhood of a quercetin molecule, the Fe−quercetin complex would be initially formed. Concerning the electronic characteristics, the Zn−quercetin bonding energy states are located between −4 eV to −3 eV, similarly to the Fe−quercetin.[6] At the Fermi level, the Zn−quercetin's spin down WF is on the quercetin, in line with the Cu−quercetin complex, while the spin up WF is

dx.doi.org/10.1021/jp509752s | J. Phys. Chem. B 2015, 119, 83−95

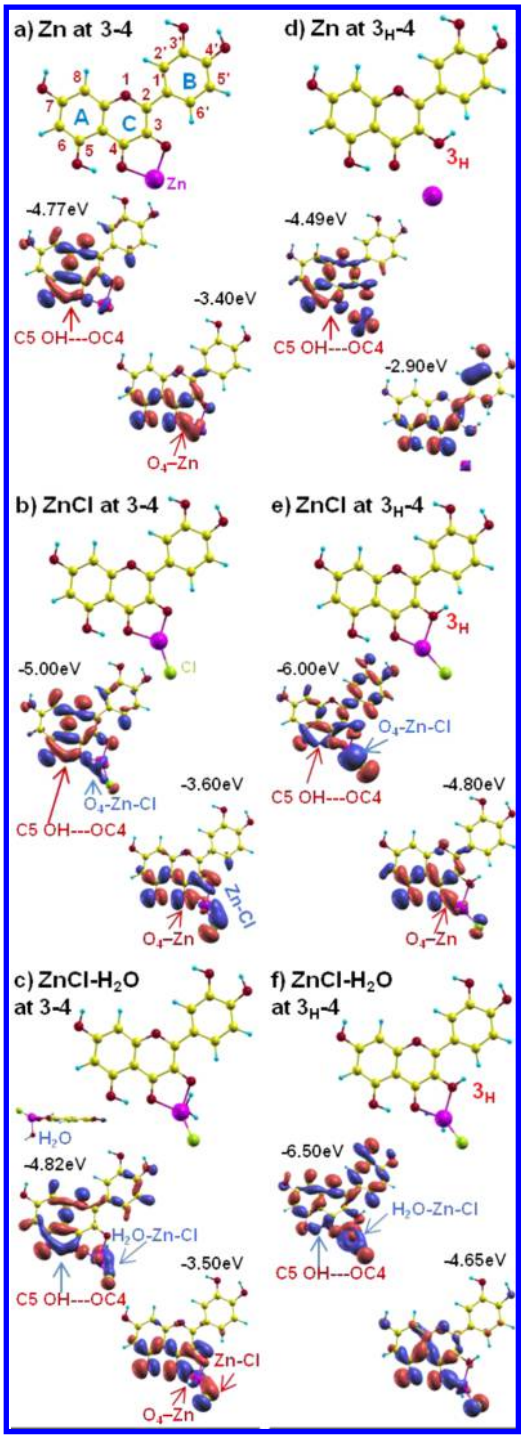

Figure 7. Zn-Quercetin complexes along with selective wave functions. The first column corresponds to the deprotonated favored 3−4 site (a, b, c) while the second one to the neural cases (d, e, f) in chlorine reservoir or not. The WF's isovalue is set from −0.1 (red) up to +0.1 (blue) e/Å^3 for the deprotonated cases while the half isovalues were used in the neutral states for the visual representation of the C-5 OH−OC-4 intramolecular hydrogen bond.

localized at the Zn site revealing s-character, similarly to the Fe−quercetin case and the Cu−quercetin state at −0.85 eV. Finally, it should be noted that the C-5 O$^-$−OC-4 intramolecular hydrogen bond that was found in the Zn−quercetin complex, Figure 7, is expected to exist also for the Fe− and Cu−quercetin complexes far from E_F.

3.2.1. Benchmark of XC Functionals. In order to explore the performances of several exchange and correlation XC functionals in reproducing the experimental results, either hybrid, such as B3LYP and M05-2X, or range-separated hybrid functionals, like wB97XD, were employed and compared with the MP2 results, as well as with those come out from both LDA and GGA calculations. All possible coordination sites of Zn(II) with both quercetin and luteolin have been explored. M05-2X optimized geometries are reported in Figure 8, while selected optimized geometries resulting from the other calculations are reported in the Supporting Information.

In Table 4, the relative stabilities of the complexes (ΔG in kcal/mol) in solution (DMSO) are presented. The most stable complexes, either neutral or deprotonated, which are the equivalent complexes in which an OH (in different position) is deprotonated, are reported as 0.00 kcal/mol in order to highlight the difference of energy between the most stable structure of each complex and the other ones.

Among the neutral quercetin complexes, employing all the XC functionals, the 4−5$_H$ site appears to be the most probable one, although the 3$_H$−4 site is unstable by less than 1 kcal/mol. Otherwise, a most noticeable difference has been found at the MP2 level of theory, since the 4−5$_H$ site is less stable by about 6 kcal/mol compared to the 3$_H$−4 one. LDA follows the majority of the XC functionals revealing the 4−5$_H$ site as the energetically favored for the neutral Zn−quercetin case against the GGA results which predict the 3$_H$′−4$_H$′ site.

Regarding the 3$_H$′−4$_H$′ Zn−quercetin complexes an interesting difference between the explored XC functionals has been found. By employing the B3LYP functional all the attempts to find a stable structure in which the Zn(II) atom lies near both the 3′OH and 4′OH quercetin sites failed. A different behavior has been observed when both M05-2X and wB97XD functionals (which include an empirical dispersion) have been used to perform the optimization calculations (see Figures S1 of the Supporting Information). Both XC functionals have been able to locate a minimum of such type, however, while at the M05-2X level its instability with respect to the most stable Zn(II) binding was found to be only 4.2 kcal/mol, at the wB97XD level a difference of 37.0 kcal/mol was calculated. This is probably due to the different binding mode of Zn(II) to the 3$_H$′−4$_H$′ site of the quercetin. In the former case it lies approximately at the same distance from both oxygen atoms (see Table 5), while in the latter one, not only the metal ion is quite far from both the O atoms but also the distance from them differs by about 0.3 Å. Similarly, in the GGA approximation Zn lies at distances 2.60 (O$_{3'}$)−2.65 (O$_{4'}$) Å that are larger than the corresponding LDA distances (2.18 (O$_{3'}$)−2.42(O$_{4'}$) Å). Anyhow, regardless of the XC functional employed, such binding type of Zn(II) to the neutral quercetin can be excluded as a coordination site.

The stability of the deprotonated quercetin complexes follows approximately the same trend than that found for the neutral ones. In this case, while at the DFT level the difference in stability of the 3−4 and 4−5 sites is at most 1.5 kcal/mol, at the MP2 level of theory the energy difference between the two most probable binding sites appears to be approximately 5 kcal/mol. In contrast to the neutral complexes, at the B3LYP level, the coordination of Zn(II) to deprotonated quercetin in both 3′ and 4′ positions was found to be much more unstable in respect to the first ones, while at the other levels of theory they lie at most 8 kcal/mol higher in energy with respect to the most stable one. LDA and GGA calculations also demonstrate

dx.doi.org/10.1021/jp509752s | J. Phys. Chem. B 2015, 119, 83−95

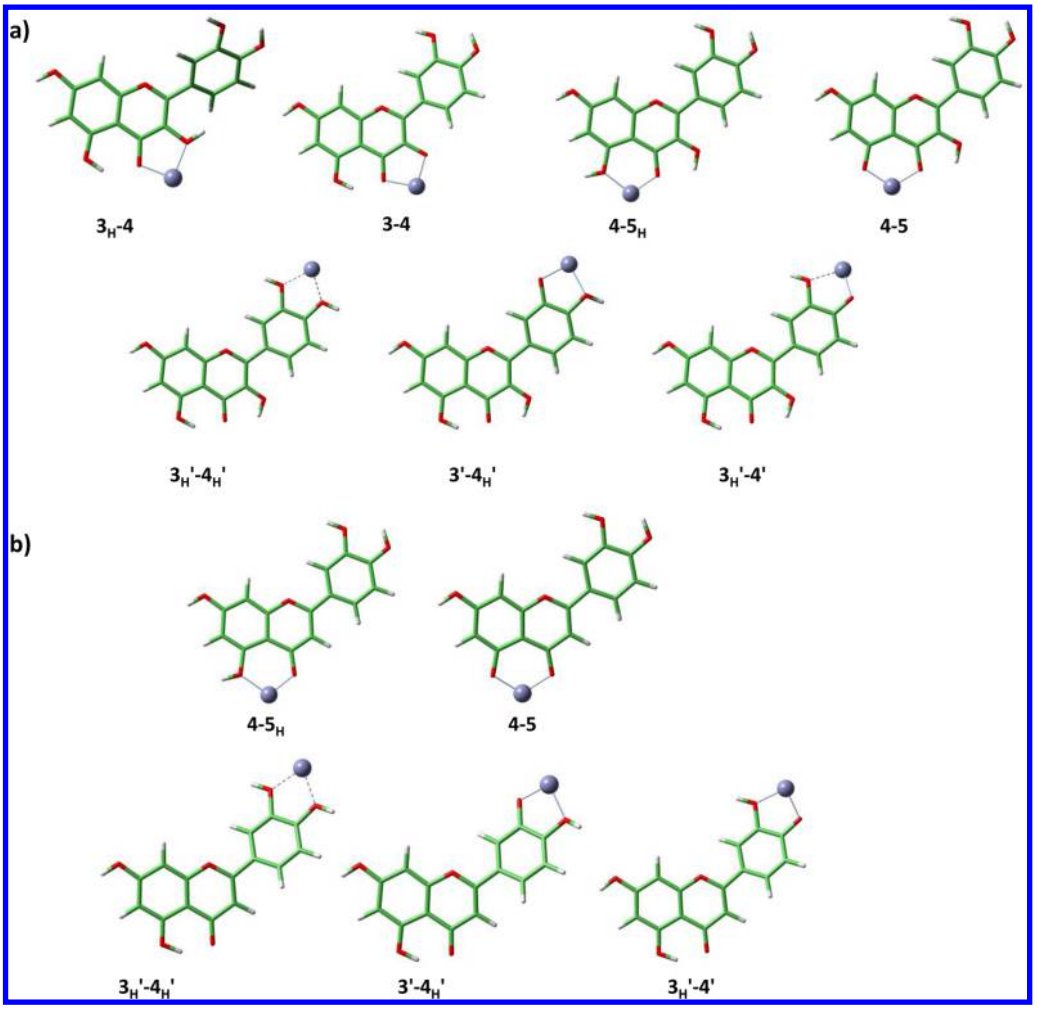

Figure 8. M05-2X optimized geometries of (a) Zn:quercetin and (b) Zn:luteolin complexes.

Table 4. Relative Stabilities (ΔG in kcal/mol) of Various Zn−Flavonoid Complexes[a]

complex	site	M05-2X	wB97XD	B3LYP	MP2	GGA	LDA
Zn:Que	3_H−4	0.3	0.5	0.9	0.0	27.7	1.4
	4−5_H	0.0	0.0	0.0	6.2	16.3	0.0
	$3_H'$−$4_H'$	4.2	37.0	–	9.3	0.0	2.0
	3−4	0.0	0.9	0.0	0.0	0.0	0.0
	4−5	0.7	0.0	1.5	4.9	7.3	16.9
	$3_H'$−4′	4.5	6.9	20.4	7.9	15.4	14.2
	3′−$4_H'$	5.7	6.2	13.4	7.9	4.9	11.2
Zn:Lut	4−5_H	0.0	0.0	0.0	0.0	18.1	18.8
	$3_H'$−$4_H'$	2.8	5.9	23.4	0.6	0.0	0.0
	4−5	0.0	0.0	0.0	0.0	6.5	0.0
	$3_H'$−4′	7.0	6.3	11.6	1.2	0.0	0.8
	3′−$4_H'$	4.3	5.1	12.5	0.3	2.3	1.9

[a]H atoms are abstracted from the OH binding sites unless denoted with a subscript H.

that the 3−4 site is the energetically favored for the deprotonated quercetin complexes, in line with the experimental NMR data.

On the other hand, luteolin can bind the Zn(II) ion through two possible sites, 4−5_H and $3_H'$−$4_H'$. Whatever the XC functional employed, the coordination 4−5_H of neutral luteolin appears to be the most probable one. In particular, while at both M05-2X and wB97XD levels of theory and the MP2 one the discrepancy in energy between the two binding modes of metal ion to the luteolin is rather small, by employing the B3LYP functional, the destabilization of the $3_H'$−$4_H'$ coordination site has been found to be 23.4 kcal/mol. Comparing the optimized structures (see Figure S2 of the Supporting Material), the only differences between them were found in both the dihedral angle intercepted by C3, C2, C1′, and C6′ atoms and the Zn binding (see Table 5). Indeed, while in the B3LYP structure the ring B is twisted by only −7.2° in respect to the plane intercepted by the condensed rings A and

dx.doi.org/10.1021/jp509752s | J. Phys. Chem. B 2015, 119, 83−95

Table 5. Selected Structural Parameters, d_{Zn-O} (Å) and θ (deg), of Zn−Flavonoid Complexes

		$d_{Zn-Ox}-d_{Zn-Oy}$;[a] θ[b]		
complex	site	M05-2X	wB97XD	B3LYP
Zn-Que	3_H-4	1.969−1.858; 37.4	1.982−1.845; 36.7	2.191−1.936; 32.6
	$4-5_H$	1.798−1.912; −0.9	1.789−1.915; 0.8	1.927−2.161; −6.1
	$3_H'-4_H'$	2.152−2.157; −7.2	3.427−3.112; 0.8	–
	3−4	1.839−1.880; −6.2	1.832−1.879; 5.5	1.931−1.983; 10.3
	4−5	1.832−1.802; −0.2	1.824−1.794; 2.8	1.835−1.806; 0.6
	$3_H'-4'$	2.105−1.877; 2.5	2.216−1.894; 2.0	3.100−2.014; −0.2
	$3'-4_H'$	1.838−2.022; 3.8	1.838−2.064; 1.2	1.942−2.506; 5.0
Zn-Lut	$4-5_H$	1.796−1.918; −1.0	1.789−1.924; 1.0	1.876−2.078; −5.1
	$3_H'-4_H'$	2.058−2.058; −25.8	2.178−2.189; −18.3	2.494−2.489; −7.2
	4−5	1.828−1.804;-3.3	1.821−1.797; 9.5	1.831−1.809; 1.3
	$3_H'-4'$	2.012−1.838; −18.0	2.052−1.836; −19.5	2.478−1.957; −6.7
	$3'-4_H'$	1.819−1.978; −24.6	1.819−2.020; −23.7	1.931−2.401; −6.0

[a]Distance of Zn from both oxygen atoms ($x-y$) of a given site. [b]Dihedral angle intercepted by C3, C2, C1′, and C6′ atoms.

Table 6. Calculated (δ_{calc}), Scaled (δ_{scaled}), and Experimental (δ_{exp}) Chemical Shifts (ppm), Mean Absolute Deviations (MAD), and Mean Deviations (ε) of Free and Zn(II)-Complexed Quercetin and Luteolin

	quercetin								luteolin							
	free				complex				free				complex			
	δ_{exp}	δ_{calc}[a]	δ_{scaled}[b]	ε[c]	δ_{exp}	δ_{calc}[a]	δ_{scaled}[b]	ε[c]	δ_{exp}	δ_{calc}[a]	δ_{scaled}[b]	ε[c]	δ_{exp}	δ_{calc}[a]	δ_{scaled}[b]	ε[c]
C2	147.2	144.0	148.6	−1.4		148.6	153.5		164.8	161.0	166.7	1.9	163	161.8	167.5	4.5
C3	136	135.3	139.3	−3.3	145.1	140.8	145.1	0.0	104.5	102.1	103.9	−0.6	107.3	101.3	103.1	−4.2
C4	176.5	165.1	171.0	5.5	178	166.8	172.8	5.2								
C5	161.4	154.9	160.2	1.2	160.1	155.5	160.8	−0.7	162.6	158.7	164.2	1.6				
C6	98.8	95.5	96.9	1.9	98.6	96.0	97.5	1.1	99.8	95.4	96.8	−3.0				
C7	164.2	155.7	160.9	3.3	163.7	157.8	163.2	0.5	164.9	157.6	163.0	−1.9	164.6	158.2	163.7	−0.9
C8	93.9	92.8	94.0	−0.1	93.7	92.2	93.5	0.2	94.4	91.3	92.5	−1.9	90.2	92.5	93.7	3.5
C9	156.4	155.2	160.5	−4.1	159.8	150.7	155.7	4.1	158.2	154.3	159.5	1.3	160.2	155.9	161.1	0.9
C10	103.7	106.6	108.8	−5.1	102.9	100.9	102.7	0.2	104.1	103.7	105.7	1.6	103.6	104.9	107.0	3.4
C1′	122.3	121.2	124.3	−2.0	125.07	120.2	123.3	1.8	122.3	121.4	124.4	2.1	122.3	116.9	119.7	−2.6
C2′	115.3	111.9	114.4	0.9	114.2	107.5	109.8	4.4	116.9	110.5	112.9	−4.0	116.9	109.1	111.4	−5.5
C3′	145.5	142.2	146.6	−1.1	145.7	139.1	143.3	2.4	150.5	140.7	145.0	−5.5	150.1	139.6	143.8	−6.3
C4′	148	142.7	147.1	0.9	146.8	145.3	149.9	−3.1	146.6	143.9	148.4	1.8	146.7	147.4	152.2	5.5
C5′	115.4	112.8	115.4	0.0	114.2	111.4	113.8	0.4	114.3	113.1	115.7	1.4	114.3	112.9	115.5	1.2
C6′	120.2	116.3	119.0	1.2	119.5	124.1	127.3	−7.8	119.9	117.2	120.1	0.2	119.4	120.5	123.5	4.1
MAD				2.1[d]				2.2[d]				2.1[d]				3.5[d]

[a]$\delta_{calc} = \sigma_{TMS} - \sigma_{calc}$. [b]$\delta_{scaled} = 1.06\ \delta_{calc} - 4.60$. [c]Mean deviation $\varepsilon = \delta_{exp} - \delta_{scaled}$. [d]Mean absolute deviation = $\Sigma|\delta_{exp} - \delta_{scaled}|/n$ (n is the number of compared chemical shift).

C, in both the M05-2X and wB97XD structures such distortion appears quite marked. Furthermore, in the B3LYP optimized structure both the distances Zn−O are longer than those found in the other complexes. While both LDA and GGA exhibit the preference of the $3_H'-4_H'$ site against the $4-5_H$ site.

A similar behavior has been found for the deprotonated Zn−luteolin complexes. Also in this case, the binding of Zn(II) on the 4−5 site of the deprotonated luteolin is the most probable one. The coordination of Zn(II) to both $3_H'-4'$ and $3'-4_H'$ sites leads to a destabilization of the complex by about 4−7 kcal/mol, with the exception of the B3LYP functional which estimates a difference in energy of such complexes of more than 11 kcal/mol with respect to the 4−5 site. In addition, while the LDA confirms the 4−5 site as preferred one, the GGA reveals the $3_H'-4'$ site. From the analysis of the optimized structures, similarly to the neutral complexes, some structural differences have been found (see Figure S3 of the Supporting Information). While both M05-2X and wB97XD XC functionals show a strong Zn(II) binding to both $3_H'-4'$ and $3'-4_H'$ sites which entails an opening of the dihedral angle θ (see Table 5), at the B3LYP level a very weak coordination of quercetin to the Zn(II) through such sites was found. Indeed, in the latter case the quercetin structure remains approximately planar and both the Zn−O distances are longer than those computed with the other functionals; consequently, a more evident destabilization of such coordination mode was found.

In contrast to the DFT results, at the MP2 level of theory the energy difference between the deprotonated 4−5 and the $3'-4'$ sites is quite small with the latter site less stable (approximately 1 kcal/mol) than the first one.

In all the examined cases both M05-2X and wB97XD, that include empirical dispersion, well reproduce the trend described by both MP2 results and NMR experiments, as well as that found with LDA calculations.

3.2.2. Theoretical Evaluation of ^{13}C Chemical Shifts. As suggested in more and less recent literature,[51,52] B3LYP functional has been selected to simulate the NMR chemical shifts of both free and complexed quercetin and luteolin species. Among the investigated complexes only for those resulted the most stable ones, on the basis of both NMR and

dx.doi.org/10.1021/jp509752s | J. Phys. Chem. B 2015, 119, 83−95

DFT outcomes, such calculations have been made. Thus, the complexes in which Zn(II) lies in site 3 and 1 of deprotonated quercetin and luteolin, respectively have been investigated.

In Table 6 and Tables S4 and S5 of the Supporting Information are collected the ^{13}C chemical shifts came out from theoretical calculations at both B3LYP/6-31+G* and B3LYP/6-311++G** levels of theory for free flavonoids and the correspondent Zn(II) complexes. The reported chemical shifts have been determined by referring the computed isotropic ^{13}C magnetic shieldings to that of TMS, which is a standard reference compound used for experimental NMR chemical shift measurements. Note that in all the considered cases we use the reference value for TMS determined at the same level of theory. Indeed, it is known that the conversion of the calculated magnetic shieldings into chemical shifts relative to a standard benefits from a systematic error cancelation.[53] All the calculated chemical shifts (δ_{calc}) were scaled (δ_{scaled}) via a scaling factor determined with a regression analysis of the calculated values and their respective experimental values (δ_{exp}) of all the investigated compounds.

As the outcomes of GIAO calculations show that increasing the size of the basis set do not change the theoretical predictions significantly, in Figure 9 has been included only the

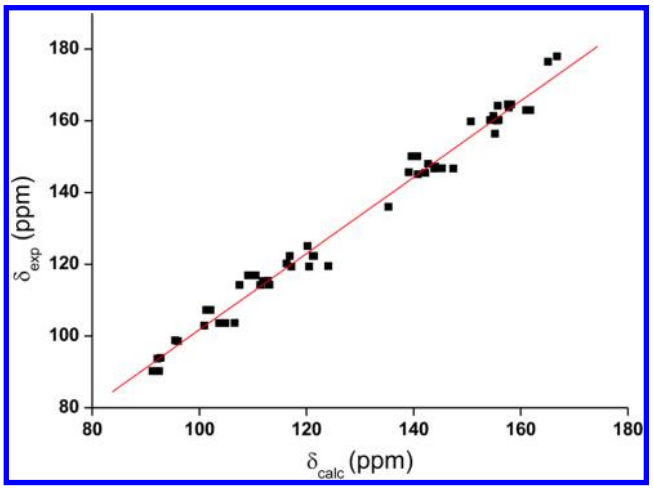

Figure 9. Linear regression plot used to determine ^{13}C NMR scaling factor. Linear fit gave $\delta_{scaled} = 1.06\delta_{calc} - 4.60$ with an R^2 value of 0.9823. Experimental (δ_{exp}) and B3LYP/6-31+G* calculated (δ_{calc}) chemical shifts are reported in ppm.

correlation between the experimental and the calculated ^{13}C chemical shifts of the considered compounds at B3LYP/6-31+G* level of theory. While that obtained at the other considered level of theory, B3LYP/6-311++G**, is reported in Figure S6 of Supporting Information.

In Table 6 are collected the ^{13}C chemical shifts computed at B3LYP/6-31+G* level of theory for free and complexed flavonoids, together with experimental and scaled counterparts.

As can be seen in Figure 9, the ^{13}C chemical shift predictions are of excellent quality as a good linear relationship is observed, with a squared correlation coefficient $R^2 = 0.9823$ and a slope of −1.0635 that is very close to the optimal value of −1.

The mean absolute deviation for free flavonoids was found to be 2.1 ppm in both cases, while a MAD of 2.2 and 3.5 ppm was obtained for Zn(II)-complexed quercetin and luteolin, respectively. Whereas, a maximum deviation of 5.5 and −7.8 ppm was found for free and complexed quercetin, respectively, which corresponds to the chemical shift of C4 in the free quercetin and C6′ in the complexed one. In the case of luteolin, the maximum deviations were found to be −5.5 and −6.3 ppm, for free and complexed species, respectively corresponding to the C3′ chemical shift in both cases.

Overall theoretical values are consistent with the experimental results and there are no large anomalies, as all the estimated chemical shifts fall within an error of a few parts per million.

4. CONCLUSIONS

In this work the Zn(II) chelation with the natural flavonoids quercetin and luteolin was investigated by the use of NMR spectroscopy and various levels of ab initio calculations. Very sharp phenolic OH ^1H resonances have been observed for both free and complexed quercetin and luteolin in DMSO-d_6 which allowed for the first time the unequivocal assignment with the combined use of $^1H-^{13}C$ HSQC and HMBC experiments. Complexation sites were found to be the CO-4 carbonyl oxygen and the deprotonated C-3 OH group of quercetin and CO-4 carbonyl oxygen and the deprotonated C-5 OH group of luteolin. Distinct resonances have been observed over a sufficiently wide range of temperatures for the free and complexed quercetin which allowed: (i) the determination of $\Delta\delta/\Delta T$ temperature coefficient of the C-5 OH proton which demonstrated that the strong C-5 OH−OC-4 intramolecular hydrogen bond persists also in the Zn(II) complex and (ii) the determination of the $\Delta H°$ and $\Delta S°$ values with $T\Delta S°$ value playing a significant role at 298 K. A linear plot of the diffusion constants of DMSO, TMS, hexamethylcyclotrithyloxane and free quercetin has been obtained with the use of DOSY experiments. This allowed the determination of the effective molecular weight of the complex which was demonstrated to be mainly 1:1 metal:quercetin.

DFT calculations demonstrated that (i) the energetically favored Zn chelation sites were found to be the CO-4 carbonyl oxygen and the deprotonated C-3 OH group of quercetin or the deprotonated C-5 OH group of luteolin against the neutral cases and other available sites, especially in the chlorine reservoir, in line with the experimental results; (ii) the experimentally observed C-5 OH−OC-4 intramolecular hydrogen bond in the deprotonated quercetin complexes was found at well localized states (below −5.5 eV from EF), and (iii) the Zn:quercetin bonding states are around −3.5 eV while antibonding states exist only close to the EF, indicating stability of these complexes.

From the benchmark of the exchange and correlation functionals, performed taking into account the solvent used in the NMR experiments, both M05-2X and wB97XD have emerged as good functionals to describe the coordination mode of both quercetin and luteolin to the Zn(II) center, although in some cases more than one coordination site of quercetin has been found to be almost equally stable.

Isotropic ^{13}C NMR shieldings from GIAO calculations account well for relative chemical shifts even with modest basis sets (such as 6-31+G*), especially if an empirical scaling is applied. Anyhow, we found that both used basis sets, 6-31+G* and 6-311++G**, give a good agreement with our reference set of experimental ^{13}C shifts.

Therefore, the combined use of NMR spectroscopy, with emphasis on the phenolic OH resonances, with ab initio calculations could provide a valuable tool for accurate structural

dx.doi.org/10.1021/jp509752s | J. Phys. Chem. B 2015, 119, 83−95

and electronic description of flavonoid−metal diamagnetic complexes.

■ ASSOCIATED CONTENT

Supporting Information

Optimized structures for the chelation of Zn(II) to the $3_H'-4_H'$ site of quercetin computed with M05-2X and wB97XD, optimized structures for the chelation of Zn(II) to the $3_H'-4_H'$ site of luteolin computed with M05-2X, wB97XD, and B3LYP, optimized structures for the chelation of Zn(II) to both the $3'-4_H'$ and $3_H'-4'$ sites of quercetin computed with M05-2X, wB97XD and B3LYP, ^{13}C chemical shifts for the free and complexed form of quercetin with Zn(II) computed at B3LYP/6-311++G** level of theory, ^{13}C chemical shifts for the free and complexed form of luteolin with Zn(II) computed at B3LYP/6-311++G** level of theory, and a plot of experimental (δ_{exp}) and B3LYP/6-311++G** calculated (δ_{calc}) chemical shifts correlations. This material is available free of charge via the Internet at http://pubs.acs.org.

■ AUTHOR INFORMATION

Corresponding Authors

*(G.M.) E-mail: gloria.mazzone@unical.it. Telephone: +390984493342 Fax: +300984493390.

* (I.P.G.) E-mail: igeroth@uoi.gr. Telephone: +302651008389. Fax: +302651008799.

Author Contributions

The manuscript was written through contributions of all authors. All authors have given approval to the final version of the manuscript. All the authors contributed equally.

Notes

The authors declare no competing financial interest.

■ ACKNOWLEDGMENTS

This research has been cofinanced by the European Union [European Social Fund (ESF)] and Greek national funds through the Operational Program "Education and Lifelong Learning" of the National Strategic Reference Framework (NSRF)—Research Funding Program: Heracleitus II investing in knowledge society through the European Social Fund. Support from the University of Calabria is gratefully acknowledged.

■ REFERENCES

(1) Rice-Evans, C. Flavonoids and Isoflavones: Absorption, Metabolism, and Bioactivity. *Free Radical Biol. Med.* **2004**, *36*, 827−828.

(2) Rice-Evans, C.; Miller, N.; Paganga, G. Structure-Antioxidant Activity Relationships of Flavonoids and Phenolic Acids. *Free Radical Biol. Med.* **1996**, *20*, 933−956.

(3) Pannala, A. S.; Chan, T. S.; O'Brien, P. J.; Rice-Evans, C. Flavonoid B-Ring Chemistry and Antioxidant Activity: Fast Reaction Kinetics. *Biochem. Biophys. Res. Commun.* **2001**, *282*, 1161−1168.

(4) Soobrattee, M. A.; Neergheen, V. S.; Luximon-Ramma, A.; Aruoma, O. I.; Bahorun, T. Phenolics as Potential Antioxidant Therapeutic Agents: Mechanism and Actions. *Mutat. Res.* **2005**, *579*, 200−213.

(5) Melidou, M.; Riganakos, K.; Galaris, D. Protection Against Nuclear DNA Damage Offered by Flavonoids in Cells Exposed to Hydrogen Peroxide: The Role of Iron Chelation. *Free Radical Biol. Med.* **2005**, *39*, 1591−1600.

(6) Ren, J.; Meng, S.; Lekka, C. E.; Kaxiras, E. Complexation of Flavonoids with Iron: Structure and Optical Signatures. *J. Phys. Chem. B* **2008**, *112*, 1845−1850.

(7) Leopoldini, M.; Russo, N.; Chiodo, S.; Toscano, M. Iron Chelation by the Powerful Antioxidant Flavonoid Quercetin. *J. Agric. Food Chem.* **2006**, *54*, 6343−6351.

(8) Kazazica, S. P.; Butkovica, V.; Srzica, D.; Klasinc, L. Gas-Phase Ligation of Fe and Cu^+ Ions with Some Favonoids. *J. Agric. Food Chem.* **2006**, *54*, 8391−8396.

(9) Guo, M.; Perez, C.; Wei, Y.; Rapoza, E.; Su, G.; Bou-Abdallah, F.; Chasteen, N. D. Iron-Binding Properties of Plant Phenolics and Cranberry's Bio-Effects. *Dalton Trans.* **2007**, *21*, 4951−4961.

(10) Zhou, J.; Wang, L. F.; Wang, J. Y.; Tang, N. Synthesis, characterization, antioxidative and antitumor activities of solid quercetin rare earth(III) complexes. *J. Inorg. Biochem.* **2011**, *83*, 41−48.

(11) Song, Y.; Leonard, S. W.; Traber, M. G.; Ho, E. Zinc Deficiency Affects DNA Damage, Oxidative Stress, Antioxidant Defenses, and DNA Repair in Rats. *J. Nutr.* **2009**, *139*, 1626−1631.

(12) Lapouge, C.; Dangleterre, L.; Cornard, J. P. Spectroscopic and Theoretical Studies of the Zn(II) Chelation with Hydroxyflavones. *J. Phys. Chem. A* **2006**, *110*, 12494−12500.

(13) Le Nest, G.; Caille, O.; Woudstra, M.; Roche, S.; Guerlesquin, F.; Lexa, D. Zn−Polyphenol Chelation: Complexes with Quercetin, (+)-Catechin, and Derivatives: I Optical and NMR Studies. *Inorg. Chim. Acta* **2004**, *357*, 775−784.

(14) de Souza, R. F.; De Giovani, W. F. Synthesis, Spectral and Electrochemical Properties of Al(III) and Zn(II) Complexes with Favonoids. *Spectrochim. Acta, Part A* **2005**, *61*, 1985−1990.

(15) Wu, D. H.; Shen, A. B.; Jonson, C. S. An Improved Diffusion-Ordered Spectroscopy Experiment Incorporating Bipolar-Gradient Pulses. *J. Magn. Reson. A* **1995**, *115*, 260−264.

(16) Perdew, J. P.; Zunger, A. Self-Interaction Correction to Density-Functional Approximations for Many − Electron Systems. *Phys. Rev. B: Condens. Matter Mater. Phys.* **1981**, *23*, 5048−5079.

(17) Perdew, J. P.; Burke, K.; Ernzerhof, M. Generalized Gradient Approximation Made Simple. *Phys. Rev. Lett.* **1996**, *77*, 3865−3868.

(18) Troullier, N.; Martin, J. L. Efficient Pseudopotentials for Plane-Wave Calculations. *Phys. Rev. B: Condens. Matter Mater. Phys.* **1991**, *43*, 1993−2006.

(19) Kleinman, L.; Bylander, D. M. Efficacious Form for Model Pseudopotentials. *Phys. Rev. Lett.* **1982**, *48*, 1425−1428.

(20) Junquera, J.; Paz, O.; Sanchez-Portal, D.; Artacho, E. Numerical Atomic Orbitals for Linear-Scaling Calculations. *Phys. Rev. B: Condens. Matter Mater. Phys.* **2001**, *64*, 235111.

(21) Sanchez-Portal, D.; Ordejon, P.; Artacho, E.; Soler, J. M. Density-Functional Method for Very Large Systems with LCAO Basis Sets. *Int. J. Quantum Chem.* **1997**, *65*, 453−461.

(22) Artacho, E.; Sanchez-Portal, D.; Ordejon, P.; Garcia, A.; Soler, J. M. Linear-Scaling Ab-Initio Calculations for Large and Complex Systems. *Phys. Status Solidi B* **1999**, *215*, 809−817.

(23) Soler, J.; Artacho, E.; Gale, J. D.; Garcia, A.; Javier, J.; Ordejón, P.; Sanchez-Portal, D. The SIESTA Method for Ab Initio Order-N Materials Simulation. *J. Phys.: Condens. Matter* **2002**, *14*, 2745−2779.

(24) Lekka, C. E.; Ren, J.; Meng, S.; Kaxiras, E. Structural, Electronic, and Optical Properties of Representative Cu-Flavonoid Complexes. *J. Phys. Chem. B* **2009**, *113*, 6478−6483.

(25) Gaussian 09, Revision **A.02**, Frisch, M. J.; Trucks, G. W.; Schlegel, H. B.; Scuseria, G. E.; Robb, M. A.; Cheeseman, J. R.; Scalmani, G.; Barone, V.; Mennucci, B.; Petersson, G. A.; et al. Gaussian, Inc.: Wallingford CT, 2009.

(26) Becke, A. D. Density-Functional Thermochemistry. III. The Role of Exact Exchange. *J. Chem. Phys.* **1993**, *98*, 5648−5652.

(27) Lee, C.; Yang, W.; Parr, R. G. Development of the Colle-Salvetti Correlation-Energy Formula into a Functional of the Electron Density. *Phys. Rev. B: Condens. Matter Mater. Phys.* **1988**, *37*, 785−789.

(28) Zhao, Y.; Schultz, N. E.; Truhlar, D. G. Design of Density Functionals by Combining the Method of Constraint Satisfaction with Parametrization for Thermochemistry, Thermochemical Kinetics, and Noncovalent Interactions. *J. Chem. Theory Comput.* **2006**, *2*, 364−382.

(29) Chai, J.-D.; Head-Gordon, M. Systematic Optimization of Long-Range Corrected Hybrid Density Functionals. *J. Chem. Phys.* **2008**, *128*, 084106.
(30) Andrae, D.; Häussermann, U.; Dolg, M.; Stoll, H.; Preuss, H. Energy-Adjusted *Ab Initio* Pseudopotentials for the Second and Third Row Transition Elements. *Theor. Chim. Acta* **1990**, *77*, 123−141.
(31) Cossi, M.; Rega, N.; Scalmani, G.; Barone, V. Energies, Structures, and Electronic Properties of Molecules in Solution with the C-PCM Solvation Model. *J. Comput. Chem.* **2003**, *24*, 669−681.
(32) Marenich, A. V.; Cramer, C. J.; Truhlar, D. G. Universal Solvation Model Based on Solute Electron Density and on a Continuum Model of the Solvent Defined by the Bulk Dielectric Constant and Atomic Surface Tensions. *J. Phys. Chem. B* **2009**, *113*, 6378−6396.
(33) Weigend, F.; Häser, M. RI-MP2: First Derivatives and Global Consistency. *Theor. Chem. Acc.* **1997**, *97*, 331−340.
(34) Ahlrichs, R.; Bär, M.; Häser, M.; Horn, H.; Kölmel, C. Electronic Structure Calculations on Workstation Computers: The Program System Turbomole. *Chem. Phys. Lett.* **1989**, *162*, 165−169.
(35) Weigend, F.; Häser, M.; Patzelt, H.; Ahlrichs, R. RI-MP2: Optimized Auxiliary Basis Sets and Demonstration of Efficiency. *Chem. Phys. Lett.* **1998**, *294*, 143−152.
(36) Schäfer, A.; Huber, C.; Ahlrichs, R. Fully Optimized Contracted Gaussian Basis Sets of Triple Zeta Valence Quality for Atoms Li to Kr. *J. Chem. Phys.* **1994**, *100*, 5829−5835.
(37) Ditchfield, R. Self-consistent perturbation theory of diamagnetism. 1. Gauge-invariant LCAO method for N.M.R. chemical shifts. *Mol. Phys.* **1974**, *27*, 789−807.
(38) London, F. J. The quantic theory of inter-atomic currents in aromatic combinations. *Phys. Radium* **1937**, *8*, 397−409.
(39) Exarchou, V.; Troganis, A.; Gerothanassis, I. P.; Tsimidou, M.; Boskou, D. Do Strong Intramolecular Hydrogen Bonds Persist in Aqueous Solution? Variable Temperature Gradient ^{1}H, ^{1}H-^{13}C GE-HSQC and GE-HMBC NMR Studies of Flavonols and Flavones in Organic and Aqueous Mixtures. *Tetrahedron* **2002**, *58*, 7423−7429.
(40) Eigen, M. Proton Transfer, Acid-Base Catalysis, and Enzymatic Hydrolysis. Part I: Elementary Processes. *Angew. Chem., Int. Ed.* **1964**, *3*, 1−19.
(41) Charisiadis, P.; Exarchou, V.; Troganis, A.; Gerothanassis, I. P. Exploring the "Forgotten" −OH NMR Spectral Region in Natural Products. *Chem. Commun.* **2010**, *46*, 3589−3591.
(42) Charisiadis, P.; Primikyri, A.; Exarchou, V.; Tzakos, A.; Gerothanassis, I. P. Unprecedented Ultra-High-Resolution Hydroxy Group ^{1}H NMR Spectroscopic Analysis of Plant Extracts. *J. Nat. Prod.* **2011**, *74*, 2462−2466.
(43) Gerothanassis, I. P. Oxygen-17 NMR Spectroscopy: Basic Principles and Applications (Part I). *Prog. Nucl. Magn. Reson. Spectrosc.* **2010**, *56*, 95−197.
(44) Gerothanassis, I. P. Oxygen-17 NMR Spectroscopy: Basic Principles and Applications (Part II). *Prog. Nucl. Magn. Reson. Spectrosc.* **2010**, *57*, 1−110.
(45) Álvarez-Diduk, R.; Ramírez-Silva, M. T.; Galano, A.; Merkoçi, A. Deprotonation Mechanism and Acidity Constants in Aqueous Solution of Flavonols: A Combined Experimental and Theoretical Study. *J. Phys. Chem. B* **2013**, *117*, 12347−12359.
(46) Kontogianni, V.; Charisiadis, P.; Primikyri, A.; Pappas, C. G.; Exarchou, V.; Tzakos, A.; Gerothanassis, I. P. Hydrogen Bonding Probes of Phenol −OH Groups. *Org. Biomol. Chem.* **2013**, *11*, 1013−1025.
(47) Charisiadis, P.; Kontogianni, V. G.; Tsiafoulis, C. G.; Tzakos, A. G.; Siskos, M.; Gerothanassis, I. P. ^{1}H-NMR as a Structural and Analytical Tool of Intra- and Intermolecular Hydrogen Bonds of Phenol-Containing Natural Products and Model Compounds. *Molecules* **2014**, *19*, 13643−13682.
(48) Siskos, M. G.; Kontogianni, V.; Tsiafoulis, C. G.; Tzakos, A.; Gerothanassis, I. P. Investigation of Solute-Solvent Interactions in Phenol Compounds: Accurate Ab Initio Calculations of Solvent Effects on ^{1}H NMR Chemical Shifts. *Org. Biomol. Chem.* **2013**, *11*, 7400−7411.
(49) Jeffrey, G. A.; Saenger, W. *Hydrogen Bonding in Biological Structures*; Spinger Verlag: Berlin, 1991.
(50) Cohen, Y.; Avram, L.; Frish, L. Diffusion NMR Spectroscopy in Supramolecular and Combinatorial Chemistry: An Old Parameter-New Insights. *Angew. Chem., Int. Ed.* **2005**, *44*, 520−554.
(51) James, R.; Cheeseman, J. R.; Trucks, G. W.; Keith, T. A.; Frisch, M. J. A comparison of models for calculating nuclear magnetic resonance shielding tensors. *J. Chem. Phys.* **1996**, *104* (14), 5497−5509.
(52) Forsyth, D. A.; Sebag, A. B. Computed ^{13}C NMR Chemical Shifts via Empirically Scaled GIAO Shieldings and Molecular Mechanics Geometries. Conformation and Configuration from ^{13}C Shifts. *J. Am. Chem. Soc.* **1997**, *119*, 9483−9494.
(53) Zhang, Y.; Wu, A.; Xu, X.; Yan, Y. Geometric Dependence of the B3LYP-Predicted Magnetic Shieldings and Chemical Shifts. *J. Phys. Chem. A* **2007**, *111*, 9431−9437.